

Automatic Image-Driven Segmentation of Left Ventricle in Cardiac Cine MRI

YingLi Lu¹, Perry Radau¹, Kim Connelly^{1,2}, Alexander Dick³, Graham Wright¹

¹Imaging Research, Sunnybrook Health Sciences Centre, Toronto, ON, Canada

²Cardiology, St Michael's Hospital, Toronto, ON, Canada

³Cardiology, Sunnybrook Health Sciences Centre, Toronto, ON, Canada

yinglilu@gmail.com, perry.radau@gmail.com, connellyka@yahoo.ca,
Alexander.Dick@sunnybrook.ca, gawright@sten.sunnybrook.utoronto.ca

Abstract. This study investigates a fully automatic left ventricle segmentation method from cine short axis MR images. Advantages of this method include that it: 1) is image-driven and does not require manually drawn initial contours. 2) provides not only endocardial and epicardial contours, but also papillary muscles and trabeculations' contours; 3) introduces a roundness measure that is fast and automatically locates the left ventricle; 4) simplifies the epicardial contour segmentation by mapping the pixels from Cartesian to approximately polar coordinates; and 5) applies a fast Fourier transform to smooth the endocardial and epicardial contours. Quantitative evaluation was performed on the 15 subjects of the MICCAI 2009 Cardiac MR Left Ventricle Segmentation Challenge. The average perpendicular distance between manually drawn and automatically selected contours over all slices, all studies, and two phases (end-diastole and end-systole) was 2.07 ± 0.61 mm for endocardial and 1.91 ± 0.63 mm for epicardial contours. These results indicate a promising method for automatic segmentation of left ventricle for clinical use.

Keywords: cardiac, left ventricle, segmentation, MRI

1 Introduction

The automatic segmentation of the left ventricle (LV) in cine MR typically faces five challenges: 1) The difficulty of locating the left ventricle; 2) the overlap between the intensity distributions within the cardiac regions; 3) the lack of edge information; 4) the shape variability of the endocardial and epicardial contours across slices and phases; and 5) the inter-subject variability of 2), 3), 4). In this work, we investigated a novel image-driven method for the accurate, robust, fast and fully automatic LV segmentation from short axis (SAX) cine MR images. The method is expected to give robust location of LV and accurate segmentation of papillary and trabecular muscles, as well as endocardial and epicardial contours in all the phases.

Main contributions of the work are that it introduces a roundness-measure-based fast and automatic LV location technique, simplifies the epicardial contours

segmentation by mapping the pixels from Cartesian to approximately polar coordinates, and applies a fast Fourier transform to smooth the endocardial and epicardial contours. The method is fully automated and is capable of computing contours for all images in approximately 2.5 minutes with non-optimized Matlab code.

2 Materials and Methods

2.1 Datasets

15 clinical cardiac cine MRI data (4 ischemic heart failure, 4 non-ischemic heart failure, 4 LV hypertrophy and 3 normals) were used in this study. The data was provided by the MICCAI 2009 Cardiac MR LV Segmentation Challenge organizers. Refer to [1] for details of the dataset.

2.2 LV Location

This section presents method based on a roundness metric to automatically locate the LV blood pool's centroid on the middle slice in the ED phase. This method is based on the following assumptions: 1) the heart is approximately in the centre of the original image; 2) the left ventricle blood pool is more circular than the right ventricle blood pool; and 3) the blood has higher signal intensity than the myocardium (i.e., bright blood imaging). This procedure consists of five steps (refer to Fig.1):

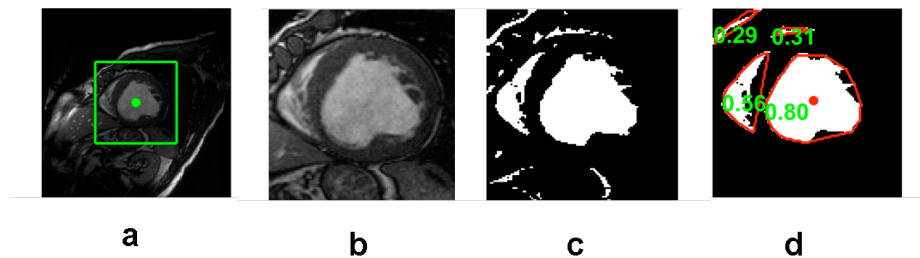


Fig. 1. LV location procedure. a. Target image with rectangular ROI (green box) and image center (green point), b. ROI image, c. Binary image, d. Surviving objects' convex hulls (red) and the corresponding roundness metric (green). The detected LV blood pool centroid is labeled as a red point.

1. Choose the middle (normally in the mid-cavity level) slice image in the ED phase as the target image.
2. Specify a centered, fixed rectangular region of interest (ROI) on the target image. The size of the rectangular is 110×110 pixels (Fig.1a, b).

3. Apply the optimal threshold method of Otsu[2] to convert the ROI to a binary image (Fig.1c).
4. Remove all objects smaller than a predefined threshold (40 pixels) and compute the convex hull of the surviving objects (Fig.1d).
5. Compute the roundness metric $R = \frac{4\pi A}{P^2}$ of each survived convex-hulled object, where, A is area and P is perimeter length. R is equal to 1 for a circle. The object with the largest roundness metric is recognized as the LV blood pool, and its centroid coordinate (x, y) is utilized for following segmentation (Fig.1d).

2.3 LV Segmentation

For each 2D image, the LV blood pool contour, endocardial contour, papillary muscles' and trabeculations' contours, and epicardial contour will be detected sequentially. Given a 2D image, the first problem is how to specify a ROI that includes the LV. Our method uses a fixed size rectangle centered on the predetermined centroid (x, y) of the LV blood pool to determine an ROI. This is based on the assumption that the central part of the LV blood pool does not move much across slices and phases.

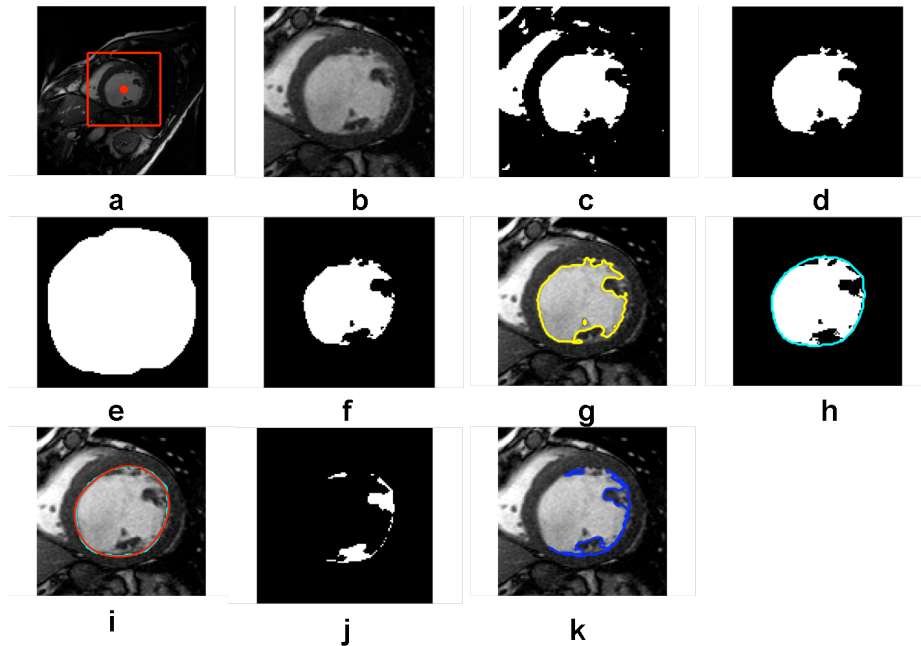


Fig. 2. LV contour calculation procedure. a. Image with rectangular ROI and previously identified LV blood pool centroid (red), b. ROI image, c. Binary image, d. Coarse LV blood pool, e. Dilated mask, f. Refined LV blood pool, g. LV blood pool contour, h. Convex hull of the LV blood pool (cyan), i. Smoothed endocardial contour (red), j. Papillary muscles and trabeculations' mask, k. Papillary muscles and trabeculations' contours (blue).

The blood pool contour is detected by the following steps (refer to Fig.2a-g):

1. Specify a rectangular ROI centered on the previously identified LV blood pool centroid coordinate (x, y) (see Section 2.2). The size of the rectangle is 110×110 pixels (Fig.2a, b);
2. Apply the optimal threshold method of Otsu[2] to convert the ROI to a binary image (Fig.2c);
3. The LV blood pool object is identified by choosing the object that has maximum overlap with a predefined mask (20×20 pixels) centered on the LV blood pool centroid (Fig.2d);
4. Dilate the LV blood pool object by a disk-shaped structuring element with radius of 20 pixels to produce a refined, smaller ROI (Fig.2e);
5. Repeat steps 2-3 based on the refined ROI. This will give a refined blood pool mask (Fig.2f).

The endocardial contour is detected by the following steps (refer to Fig.2h, i):

1. Compute the convex hull of the refined blood pool (Fig.2h);
2. Smooth the convex hull's contour by applying the 1D fast Fourier transform (FFT) [3]. We first compute the FFT of the x coordinate of the contour point index, multiply the result by a low pass filter transfer function (keep only the four lowest frequency components), then take the inverse transform to produce the smoothed x coordinate. Repeat for y coordinates (Fig.2i).

The papillary muscles' and trabeculations' contours are detected by these steps:

1. Subtract the convex-hull mask of the refined blood pool from the refined blood pool mask to calculate the mask image of the papillary muscles and trabeculations (Fig.2j);
2. Trace the exterior boundaries of the objects in the mask image to determine the papillary muscles' and trabeculations' contours (Fig.2k).

The epicardial contour is calculated by the following steps (refer to Fig.3a-f):

1. Map the pixels from Cartesian to approximately polar coordinates. An outer boundary is calculated by dilation of the endocardial contour. The two contours are interpolated to the same number of points, and paired to derive scan lines, each of a predefined length (20 pixels) (Fig. 3a). The result is a rectangular image that extends from the endocardial contour (top row) outward (bottom row) (Fig.3b).
2. Use each top-row pixel as a region growing seed, with all grown regions added and converted to a binary image (Fig.3c). For region growing, intensities are normalized by the original image maximum, and pixels added to a grown region must meet the intensity criterion (difference from mean of the grown region less than 0.04).
3. Fill image holes by morphological operations (Fig.3d).
4. The end point of each column's grown region determines an edge point (Fig.3e).
5. Inverse transform the edge point coordinates to the original coordinate space to determine the epicardial contour (Fig.3f).
6. Smooth the contour by applying the FFT technique as described earlier (Fig.3f).

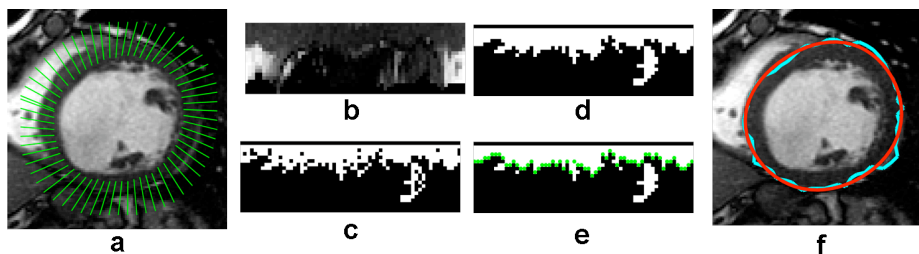


Fig. 3. LV segmentation procedure for epicardial contour. a. Scan lines for mapping the pixels from Cartesian to polar coordinates. b. Result of image transform. c. Region growing binary image. d. Image after filling holes. e. Edge points (green). f. Epicardial contour before (blue) and after FFT smoothing (red).

2.4 Evaluation

The performance of the segmentation algorithm was evaluated, both quantitatively and qualitatively according to the Challenge evaluation framework [1]. In order to quantitatively evaluate the detected endocardial and epicardial contours of the ED and ES phases of all slices several measures were assessed: average perpendicular distance (APD), the Dice metric (DM) [4], Clinical parameters (Ejection fraction(EF) and Left Ventricular Mass(LVM)). In order to qualitatively evaluate the contours, an experienced cardiologist (blinded to the participants) rated the segmentation results on a four point visual scale. In accordance with the Challenge rules, the algorithm training did not include the validation or online data sets. The algorithm was previously trained with data sets from other subjects, with similar MR scan characteristics.

3 Results

The automatic segmentation method were tested on 15 clinical MR exams. The accuracy of LV location is 93.33%(14/15). The average computation time of LV location is 0.074 ± 0.014 s per subject. The average perpendicular distance (APD) and Dice metric (DM) over slices and ES and ED phases calculated for our method are shown in Table 1. The EF and LVM are shown in Table 3, indicating only the results where the papillary muscles are included in the cavity in accordance with the expert contours. The visual assessment results are shown in Table 3. There are five studies where the algorithm has difficulty with detection of Left Ventricular Outflow Tract (LVOT), six studies with difficulty at the apex, and four studies have the problem of missing contours. For all the studies, the detected contours are very accurate.

The average computation time of the segmentation of the proposed method is 144.89 ± 44.07 s per subject including the time of reading DICOM data and saving contour files. The computation time is 0.65s per image for the the 15 exams. The computation time was tested on consumer hardware (2×2.8 GHz Quad-core Intel

Xeon Mac Pro, Apple) with a non-optimized Matlab code (Mathworks) implementation.

Table 1. Detect percentage, good percentage, APD and DM

Patient ID	Detect percentage		Good percentage		APD		DM	
	IC	OC	IC	OC	IC	OC	IC	OC
SC-HF-I-05	83.33	88.89	83.33	88.89	1.37	1.06	0.94	0.97
SC-HF-I-06	100.00	100.00	95.45	100.00	1.32	2.15	0.94	0.93
SC-HF-I-07	87.50	100.00	87.50	100.00	2.44	1.57	0.87	0.95
SC-HF-I-08	50.00	63.64	50.00	63.64	1.61	2.59	0.94	0.94
SC-HF-NI-07	87.50	91.67	87.50	91.67	2.61	1.09	0.89	0.97
SC-HF-NI-11	100.00	100.00	100.00	80.00	2.19	1.57	0.90	0.96
SC-HF-NI-31	63.16	70.00	63.16	70.00	2.41	1.51	0.90	0.96
SC-HF-NI-33	94.44	100.00	83.33	90.00	2.04	2.01	0.89	0.94
SC-HYP-06	76.92	85.71	76.92	57.14	2.30	3.26	0.85	0.90
SC-HYP-07	68.75	87.50	50.00	87.50	1.87	2.81	0.90	0.92
SC-HYP-08	63.16	80.00	42.11	80.00	3.77	1.81	0.85	0.95
SC-HYP-37	46.15	57.14	46.15	57.14	1.93	2.45	0.84	0.92
SC-N-05	66.67	75.00	53.33	75.00	1.66	1.38	0.87	0.95
SC-N-06	84.62	85.71	84.62	85.71	1.77	1.77	0.88	0.93
SC-N-07	94.44	100.00	83.33	90.00	1.79	1.63	0.89	0.93
Statistics								
Mean	77.78	85.68	72.45	81.11	2.07	1.91	0.89	0.94
Std	17.35	14.06	19.52	13.95	0.61	0.63	0.03	0.02

IC: inner contour, OC: outer contour

Table 2. Ejection Fraction and Left Ventricle Mass

Patient ID	EF(PIC)		LVM(PIC)	
	Auto	Expert	Auto	Expert
SC-HF-I-05	34.24	33.0 3	111.22	115.45
SC-HF-I-06	21.32	25.7 8	178.62	147.34
SC-HF-I-07	38.16	28.1 8	142.70	114.12
SC-HF-I-08	23.99	21.4 2	134.79	124.40
SC-HF-NI-07	23.81	12.9 1	155.99	130.54
SC-HF-NI-11	17.71	14.8 4	198.98	158.25
SC-HF-NI-31	43.88	35.5 9	126.25	127.38
SC-HF-NI-33	66.54	58.3 5	176.95	130.78
SC-HYP-06	69.55	60.4 3	78.53	91.59
SC-HYP-07	75.04	62.2 7	175.83	133.55
SC-HYP-08	NaN	58.6 9	298.08	278.17
SC-HYP-37	81.84	71.6 8	94.00	125.38
SC-N-05	82.57	62.8 1	64.49	73.50
SC-N-06	65.20	54.5	74.48	64.02

SC-N-07	61.33	9 6	59.0	112.05	102.34
Mean	50.37	8	43.9	141.53	127.79
Std	23.81	7	19.9	60.09	48.77

EF: ejection fraction, LVM: left ventricle mass, PIC: papillary included in the LV cavity

Table 3. Visual assessment

Category	HF-I	HF-NI	HYP	N	Overall
Average	1.8	2.0	2.8	1.7	2.1

4 Discussion and Conclusions

The proposed segmentation method does not need initialization by manually drawn contours, prior statistical shape model, or gray-level appearance model. The proposed method is an image-driven method with only the assumption that the LV blood pool in a short axis image is approximately circular. Therefore it should be suitable for datasets with a wide range of anatomy, function, and image contrast as required for routine clinical use.

Previous methods of LV location usually have two steps: locate the entire heart and then the LV. The proposed roundness metric method provides an alternative for locating the LV, and it requires only a single step. It is very fast, taking 0.0736 ± 0.0139 s per subject. However, analysis of the validation data sets indicates that some development is required to improve robustness.

A difficult challenge of LV segmentation is the accurate delineation of the epicardial contours. The typical problem is ballooning epicardial contours at the junction between myocardium and lung parenchyma and subdiaphragmatic tissues., caused by small intensity difference between these tissues. By mapping the pixels from Cartesian to polar coordinates, the irregular, ring-shaped ROIs are transformed to rectangular images. In this way, the epicardial contour detection problem was simplified.

Smoothing the contours by the FFT is a very fast and effective technique. The main merit of the FFT technique is to provide smoothed contours by removing outliers of the detected edge points without changing the overall shape.

The proposed method can provide contours of papillary muscles and trabeculations. Clinical studies have employed different quantification methods for calculation of LV volume, mass and ejection fraction by including or excluding papillary muscles and trabeculations in the ventricular cavity [9, 10]. Recent studies have shown that the papillary muscles and trabeculations have a significant impact on calculation of LV volume and mass [9] and ejection fraction [10]; therefore the proposed method provides additional important options for daily clinical application.

There are limitations of the proposed method: 1) it can not segment the LV from the right ventricle if the SAX slice includes the atria; 2) the small blood pool at the apex is difficult to detect correctly; and 3) there are some slices where the algorithm fails and the contours are not generated. These problems were most noticeable for the

subjects with hypertrophy. There is a need for an improved 3D or 4D (3D + phase) constraint to improve the contour detection robustness of the algorithm, and this will be the subject of future research.

For subjects where the contour detection percentage and “good” percentage (i.e. APD < 5mm) were less than 100% there were insufficient or inadequate contours, and the clinical parameters EF and LVM were not reliable for clinical purposes. However, where the contours met these criteria, the resulting EF and LVM were highly correlated with the expert values.

In summary, the proposed fully automated segmentation technique has shown promising results that merit further development for quantification of cine cardiac MR in clinical practice.

References

1. Radau P., Lu Y., Connelly K., Paul G., Dick A.J., Wright G.A.: Evaluation Framework for Algorithms Segmenting Short Axis Cardiac MRI. The MIDAS Journal-Cardiac MR Left Ventricle Segmentation Challenge, <http://hdl.handle.net/10380/3070>.
2. Otsu, N.: A Threshold Selection Method from Gray-Level Histograms, *IEEE Transactions on Systems, Man, and Cybernetics*, 9(1), 62-66(1979)
3. Gonzalez, R.C., Woods R.E., *Digital Image Processing*, second edition, New Jersey, Prentice Hall, 2001, Chapter 4
4. Lynch M., Ghita O., Whelan P.F.: Segmentation of the left ventricle of the heart in 3-D+t MRI data using an optimized nonrigid temporal model. *IEEE Trans Med Imaging*, 27(2), 195-203(2008)
5. Sorgel, W., Vaerman, V.: Automatic heart localization from 4D MRI datasets. *SPIE : Med. Imag.* 3034, 333–344(1997)
6. Lin X., Cowan B.R., Young A.A., Automated detection of left ventricle in 4D MR images: experience from a large study. *Med Image Comp Comp Assist Interv.* 9(Pt 1),728-735(2006)
7. Pednekar A., Kurkure U., Muthupillai R., Flamm S., Kakadiaris I.A.:Automated left ventricular segmentation in cardiac MRI. *IEEE Trans Biomed Eng.* 53(7), 1425-1428(2006).
8. Mitchell S.C., Lelieveldt B.P., van der Geest R.J., Bosch H.G., Reiber J.H., Sonka M.: Multistage hybrid active appearance model matching: segmentation of left and right ventricles in cardiac MR images.*IEEE Trans Med Imaging*, 20(5), 415-423(2001)
9. Papavassiliu T., Kühl H.P., Schröder M., Süsselbeck T., Bondarenko O., Böhm C.K., Beek A., Hofman M.M., van Rossum A.C.: Effect of endocardial trabeculae on left ventricular measurements and measurement reproducibility at cardiovascular MR imaging. *Radiology*. 236(1):57-64(2005)
10. Weinsaft J.W., Cham M.D., Janik M., Min J.K., Henschke C.I., Yankelevitz D.F., Devereux R.B.: Left ventricular papillary muscles and trabeculae are significant determinants of cardiac MRI volumetric measurements: effects on clinical standards in patients with advanced systolic dysfunction. *Int J Cardiol.* 126(3):359-65(2008)